Design of a Robotic Module for Autonomous Exploration and Multimode Locomotion

Sheila Russo, *Student Member, IEEE*, Kanako Harada, *Member, IEEE*, Tommaso Ranzani, *Student Member, IEEE*, Luigi Manfredi, *Member, IEEE*, Cesare Stefanini, *Member, IEEE*, Arianna Menciassi, *Member, IEEE*, and Paolo Dario, *Fellow, IEEE*

***Abstract*—The mechanical design of a novel robotic module for a self-reconfigurable modular robotic system is presented in this paper. The robotic module, named Scout robot, was designed to serve both as a fully sensorized autonomous miniaturized robot for exploration in unstructured environments and as a module of a larger robotic organism. The Scout robot has a quasi-cubic shape of 105 mm × 105 mm × 123.5 mm, and weighs less than 1 kg. It is provided with tracks for 2-D locomotion and with two rotational DoFs for reconfiguration and macrolocomotion when assembled in a modular structure. A laser sensor was incorporated to measure the distance and relative angle to an object, and image-guided locomotion was successfully demonstrated. In addition, five Scout robot prototypes were fabricated, and multimodal locomotion of assembled robots was demonstrated.**

***Index Terms*—Autonomous exploration, modular robots, multimode locomotion, self-reconfigurable robots.**

I. Introduction

ROBOTS designed for single purposes are able to accurately perform specific tasks, yet their performance tends to be poor for heterogeneous tasks in different environments. Modular robotic approaches have been investigated mainly for autonomous operation in unstructured environments. Modular robotic applications include rescue operations in earthquake regions [1], war scenarios [2], and space applications [3]. These previous studies on modular robots have demonstrated that robots with the capability to change their shape to better fit the environment and required functionality are more likely to succeed than fixed-architecture robots [4]–[6]. Self-reconfigurability is a feature enabling robots to autonomously change their shape and size to meet specific operational demands [7]. A self-reconfigurable robot is composed of autonomous mechatronic modules that can connect to, be disconnected from, and communicate with adjacent modules. Certain self-reconfigurable robots are capable of adapting shape and functions to changing environments without external help [8]; in other cases, the modules can be disconnected from the main structure and reused to create a different structure [9]. Other examples include self-reconfigurable robots which can form a snake-like shape, e.g., to move in tight spaces and reassemble to a spider-like configuration to cross uneven terrain [10], and also robots that form a ball or a wheel able to move quickly over a fairly flat terrain [1]. Thus, self-reconfigurable modular robots are versatile, fault-tolerant, and efficient [11]–[13].

Self-reconfigurable modular robots can be generally classified into two categories depending on the geometric arrangement of their modules: lattice-type robots and chain-type robots [5]. Lattice architectures have units that are arranged and connected in some regular, 3-D patterns, such as a simple cubic or hexagonal grid [4]. Lattice-type robots, such as molecule [14], are able to change their shape by moving into different positions on this virtual grid, which is the so-called lattice. Chain-type systems are composed of modules that are arranged to form single- or multibranched linkages. Both snakes and multilegged walkers are possible configurations for these systems [9]. Chain-type robots, such as PolyBot [15], CONRO [16], and M-TRAN [17], can reconfigure themselves by attaching and detaching chains of modules.

A novel robotic module named Scout robot is presented in this paper. The Scout robot is one of the three robotic modules designed for a symbiotic self-reconfigurable modular robotic system [18] [see Fig. 1(a)] and it is devoted to autonomous exploration in unstructured environments. The Scout robot is an attempt to bridge a gap between swarm robots and self-reconfiguring robots, where the technologies are often found as separate research topics. Indeed, each Scout robot, thanks to its sensors and locomotion capabilities, can move autonomously and safely on rough terrains, explore the surroundings, and interact both with the environment and with other robots [see Fig. 1(b)]. Furthermore, this platform has the capability to act also as a part of an assembled robotic organism. In fact, the Scout robot is equipped with two DoFs and four docking units; moreover, it shares the same docking design with the other robotic modules. Consequently, it can be assembled with other Scout robots or other robotic modules to form a structure and perform reconfiguration and 3-D locomotion. Thanks to on-board sensors embedded for exploration tasks, the Scout robots can be, for instance, the "eyes" of the assembled organism [see Fig. 1(c)]

Manuscript received August 25, 2011; revised February 2, 2012 and May 18, 2012; accepted July 2, 2012. Date of publication August 31, 2012; date of current version December 11, 2013. Recommended by Technical Editor G. Liu. This work was supported by the European Commission in the framework of the REPLICATOR FP7 project under European Project 216240.

S. Russo, T. Ranzani, L. Manfredi, C. Stefanini, A. Menciassi, and P. Dario are with the BioRobotics Institute, Scuola Superiore Sant'Anna, 56025 Pontedera, Italy (e-mail: s.russo@sssup.it; t.ranzani@sssup.it; c.stefanini@sssup.it; a.menciassi@sssup.it; p.dario@sssup.it).

K. Harada is with the School of Engineering, The University of Tokyo, Tokyo 113-8656, Japan (e-mail: kanako@nml.t.u-tokyo.ac.jp).

L. Manfredi is with the Institute of Medical Science and Technology, University of Dundee, Dundee, DD1 4HN, U.K. (e-mail: l.manfredi@sssup.it).

Color versions of one or more of the figures in this paper are available online at http://ieeexplore.ieee.org.

Digital Object Identifier 10.1109/TMECH.2012.2212449

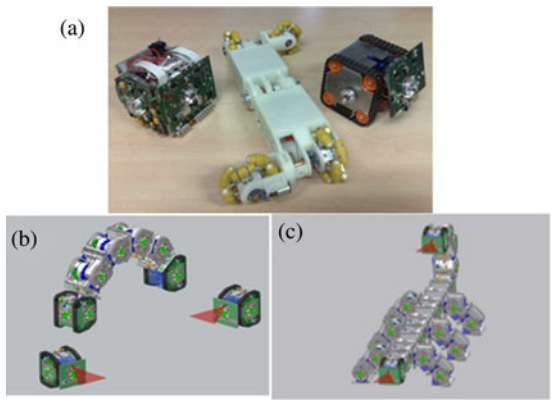

Fig. 1. Symbiotic modular robotic system: (a) prototypes of the three robotic modules for multirobot organisms (from left to right: backbone robot, active wheel, Scout robot), (b) Scout robots in the symbiotic robotic system, and (c) an example of an assembled organism (scout robots are placed at its head and tail).

or can perform other sensing functions. At any time, the Scout robot can detach from the organism thanks to its full mobility and move away to explore the surroundings using its on-board sensors. The mechanical design of the Scout robot is presented in this paper along with the experimental results of its basic performance.

This paper is organized as follows. Section II presents the requirements of the Scout robot, whereas Section III examines the mechanical design. Section IV reports performance evaluation experiments while conclusions and description of future research directions are provided in Section V.

II. Mechanical Design Overview

As specified previously, the Scout robot aims at bridging the gap between swarm robots and self-reconfiguring robots; therefore, much effort was put in its mechanical design. It had to be designed as a fully sensorized autonomous miniaturized robot for exploration in unstructured environments and, at the same time, it had to serve as a module of a self-reconfigurable modular robotic system, composed of different robotic modules for reconfiguration and macrolocomotion. In order to accomplish this goal, all requirements were investigated as summarized next.

A. General Mechanical Requirements

The Scout robot has a quasi-cubic shape: this was chosen for easy alignment of the docking units regardless of the orientation, in order to facilitate self-assembly and self-reconfiguration. The chassis has to be lightweight to allow reconfiguration and macrolocomotion when the robots are in a multirobot organism configuration, but it needs to be rigid enough to support docked robots and withstand unexpected collisions.

B. Autonomous Locomotion

Given that exploration in unstructured environments is the purpose of the Scout robot, each module needs to accommodate several battery packs to perform autonomous locomotion. For example, the Scout robot must be able to move on terrains of different texture, overcome small obstacles or holes, and climb slopes. To be effective in practical applications, locomotion has to be quick enough to explore the surroundings within a given battery charge.

C. Exploration of the Environment

On-board sensors are required to perform autonomous exploration of the environment. Each module has to be equipped with internal sensors to guarantee the autonomy of individual modules; both short- and far-range detection capabilities are required for scanning the surroundings. The Scout robot has to be able to detect obstacles or holes on the terrain during locomotion.

D. Macrolocomotion

When Scout robots are docked together or docked to other robotic modules, the assembled structure needs to perform self-reconfiguration and 3-D locomotion. Therefore, it is essential for the Scout robot module to have one or more DoFs. In addition, the Scout robot should have enough actuation torque to lift other docked modules as well.

Another robotic module of the symbiotic modular robotic system, the so-called backbone robot [see Fig. 1(a)] [18], is mainly in charge of the 3-D locomotion of assembled structures and has 1 DoF with strong actuation torque (7 Nm), while Scout robots are mainly expected to provide sensing capabilities to the assembled organism. Based on these different roles for different robots, in the Scout robot, the actuation torque should allow the platform to form small organisms for reconfiguration, macrolocomotion, and cross-over obstacles encountered during exploration tasks.

E. Docking

Docking mechanisms have to be mounted on all side walls of the Scout robot and must assure docking/undocking between individual modules as well as electrical connections for power sharing and signal transmission. As all three robotic modules must share the docking design to form a structure composed of different module types [18], a docking unit was purposely designed in the framework of the REPLICATOR project [19]. The docking unit has a symmetrical unisex design and allows low misalignment for autonomous docking and undocking.

III. Mechanical Design and Fabrication

Details on the Scout robot platform design follow. In order to meet the requirements described previously, the reported solutions were adopted.

A. General Features

The Scout robot has a quasi-cubic shape [see Fig. 2(a) and (b)], and the size of the module is 105 mm $\times$ 105 mm $\times$ 123.5 mm. It is provided with tracks for 2-D locomotion and with two rotational DoFs for reconfiguration and macrolocomotion of assembled structures. The chassis is composed of 3 mm and 4 mm thick walls [see Fig. 2(c)]. This feature facilitates easy mass production of the robots because machining of thin walls

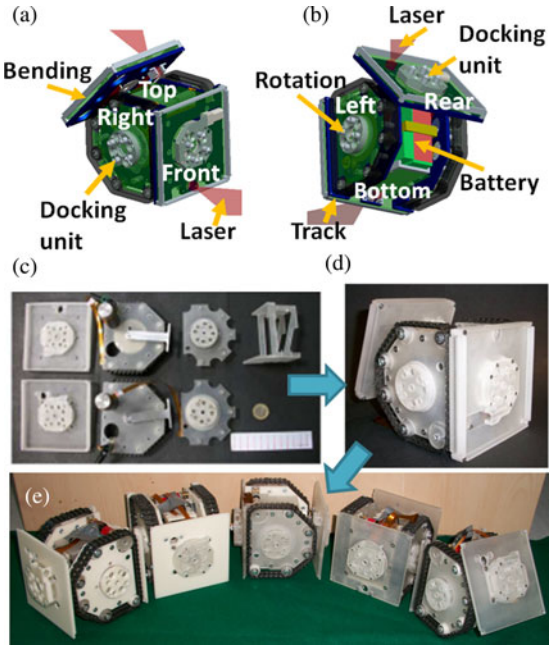

Fig. 2. Scout robot: (a) front view of the CAD model, (b) rear view of the CAD model, (c) assembly of the robot, (d) robot prototype, and (e) five prototypes fabricated.

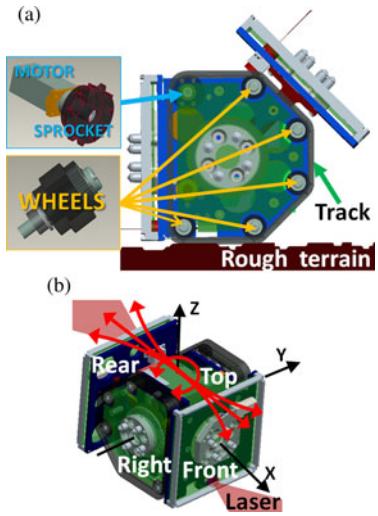

Fig. 3. Locomotion unit of the Scout robot: (a) details of the Scout robot locomotion unit and (b) locomotion capabilities (indicated by the red arrows)—move forward and backward, and turn left, right, and about its axis.

can benefit from laser-cutting or rapid prototyping technologies. All components of the Scout robot can be first assembled into small subparts [see Fig. 2(c)], and then these parts can be assembled together to form the entire robot [see Fig. 2(d)]. Five prototypes were fabricated to conduct experiments and validate basic performance. These prototypes are shown in Fig. 2(e) next to each other and opportunely oriented in order to have a complete view of the robot.

The Scout robot is lightweight because most parts are made of polymer by rapid prototyping. Only a few parts have been fabricated in metal to confer a higher stiffness to the robot. The final weight of the robot, integrating all commercial and manufactured components, is 1 kg.

The Scout robot embeds six packs of lithium batteries, each one with 1400 mAh capacity (4LI1002, TP Electronic Components GmbH, Germany). The platform design allows custom-made printed circuit boards (PCBs) to be placed on each wall [as shown in green in Fig. 2(a) and (b)]. The PCBs are going to be connected, in the future versions, to each other and to all on-board electronic components. The basic mechanical functions of the Scout robot have been validated by employing tethered control instead of wireless control using PCBs, which was convenient to rapidly and effectively test the robot's main functionalities and validate mechanical performance.

B. Locomotion Unit

Two independently driven motors (212-404, Precision Microdrives, U.K.) were integrated in each robot. Such motors are a good tradeoff between torque, speed, and small dimensions. The selected motors have an external diameter of 12 mm, a total length of 32 mm (including the shaft), and a nominal output stall torque of 336 mNm. Each motor is directly connected to a sprocket; motion is transmitted through an elastic track (Mod.70100, TAMIYA, Japan), which has small holes for the teeth, to five passive wheels, as shown in Fig. 3(a).

Thanks to its tracked locomotion, the Scout robot is able to move on challenging terrains. Indeed, by using tracks, a large surface area is in contact with ground, thus causing low ground pressure. This is an important feature if we want to move on soft terrains, where the robot could be stuck. The robot can move forward and backward, and turn left, right, and about its axis [see Fig. 3(b)], by changing the relative velocity and the moving direction of the tracks. The estimated locomotion speed is 105 mm/s approximately (1 body length per second), and the maximum slope that the robot is able to climb is 42°.

Locomotion on three planes is possible thanks to the design of the locomotion unit, as shown in Fig. 4. This capability allows locomotion even after an accidental overturning. This feature is important when the robots are undocked and separated from an organism which, for instance, performed several reconfigurations to obtain a specific topology. If the locomotion was feasible only on one surface, the organism would need to perform another reconfiguration only to place the robot on the ground and let it move away.

In addition, tracks can be exploited for locomotion of the assembled structure [see Fig. 1(b)]. This enables fast locomotion of an assembled structure on a relatively flat terrain without using the energy of the robotic modules carried by Scout robots. In this way, a chain of robotic modules, for example, can be delivered to an organism without losing energy before the assembly.

Inputs to the locomotion motors were managed using an H-bridge driver (L298, STMicroelectronics) controlled through a National Instruments USB data acquisition device (NI USB-6009) and programmed using LabVIEW. During experiments, odometry was used for locomotion control. This procedure was convenient to rapidly and effectively test the robot's locomotion performance.

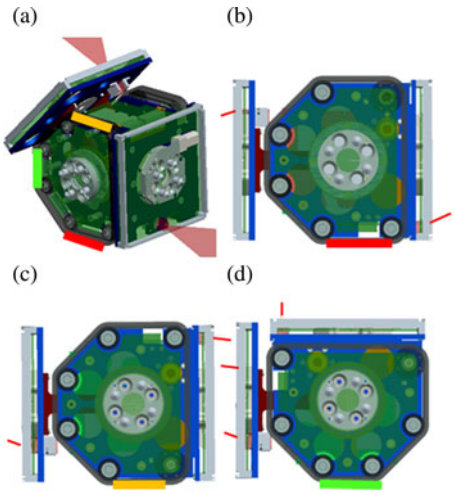

Fig. 4. Locomotion planes: (a) three planes of locomotion, (b) bottom-side plane, (c) top-side plane, and (d) locomotion on the rear-side plane at 90° bending.

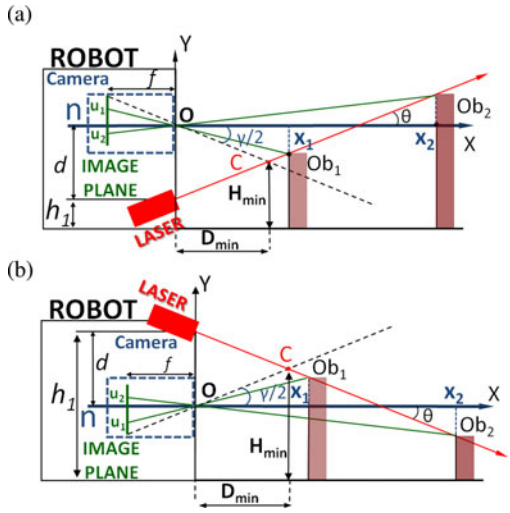

Fig. 5. Laser-camera configurations: (a) laser at bottom with an upward inclination and (b) laser on top with a downward inclination.

C. Sensing Unit

To the best of the author's knowledge, in the state of the art of swarm and modular robotics most attention has been put in sensors for low range interaction, e.g., docking, with other robots and for detection of changes in the environmental conditions (light, humidity, etc.) [20]–[23]. Some examples of robots more focused on exploration tasks can be found, but their design is much less focused in modularity, reconfigurability, and formation of robotic organisms [23]–[25]. The objective of the Scout robot is to represent a flexible platform where the integration of the exploration capabilities does not limit its performances as a self-reconfigurable modular robot. The Scout robot is a flexible robotic module where different kind of sensors can be integrated such as sensors for environmental sensing (humidity/temperature measurement, image capturing, laser scanning, etc.), locomotion control (3-D acceleration, localization, angle measurement, etc.), and internal control (voltage and current monitoring, etc.) [18]. Among these sensors, far-range sensors for environmental sensing are the most important for the Scout robot tasks. A triangulation-based laser-camera sensor was selected for this purpose as a good compromise between size, complexity, cost, functionalities, and power consumption, and the basic functionalities were tested. As widely known, the idea of triangulation laser sensors is to use a laser beam and a camera to build up a triangle together with a targeted object. The designed laser triangulation sensing unit consists of a laser-line generator (LT-1-650, Electron Ltd., Taiwan) and a miniaturized camera (OV7670, Omni Vision, IL) used for robot vision.

1) Development of Laser-Camera Sensing Units: Design and integration of the laser-camera sensor on the Scout robot is important, since the sensing capabilities change depending on laser and camera configuration. A tilted configuration of the laser diode was chosen while the camera position was fixed and not tilted for easier implementation on the corresponding PCB board. Two different configurations of the laser and the camera were implemented on Scout robot's front and rear wall, in order to integrate two different laser camera triangulation sensors. On the front wall the camera is placed above, and the laser placed below with an upward inclination as shown in Fig. 5(a). In this configuration, the sensor is mainly effective for far-range sensing and detection of relatively high objects, whereas holes or objects close to the robot cannot be detected. On the other hand, when the camera is placed below and the laser has a downward inclination as shown in Fig. 5(b), the sensor is effective for short-range sensing, and holes can be easily detected. All the obstacles that fall in such range will be anyway detected. The minimal detectable distance and the corresponding minimum height of an object can be estimated by trigonometric considerations as reported in [26]. Indeed, the front wall can detect objects higher than 85 mm from a minimal distance of 300 mm to a theoretically infinite distance. However, as reported in [26], objects farther than 600 mm are detected with a significant decrease in the accuracy. On the other hand, taking advantage of the laser sensor on the rear side, the robot can detect objects lower than 67 mm in height, in the range from 75 mm up to 600 mm from the robot. By combining the different features of the two laser-camera sensors, the robot can overturn after a definite amount of time to detect at best the presence of near- and far-range obstacles or possible holes on the floor. Considering the locomotion speed of the robot, the overturning would take approximately 0.65 s.

The laser-camera sensing units were mounted on the front wall [see Fig. 6(a)] and on the rear wall [see Fig. 6(b)] using the configuration shown in Fig. 5(a) and (b), respectively. The laser unit on the rear wall was not placed in the center so as not to hinder bending actuation. The laser-camera sensing unit on the actuating wall resulted in laser sweeping capability as shown in Fig. 6(c).

Fig. 7 shows captured images when the robot was placed at 20 and 40 cm from the wall. The configuration shown in Fig. 5(a), implemented on the front wall, demonstrated good far-range scanning as well as good detection of high objects. On the other hand, the configuration shown in Fig. 5(b) implemented on the

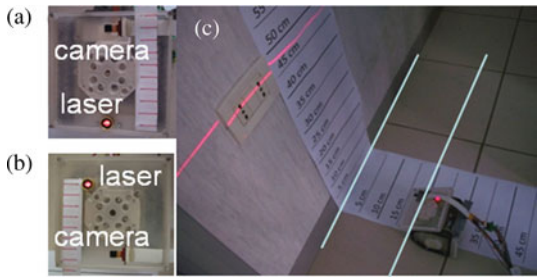

Fig. 6. Laser-camera sensing unit mounted on (a) front wall, (b) rear wall, and (c) laser sweeping by actuation of the rear wall.

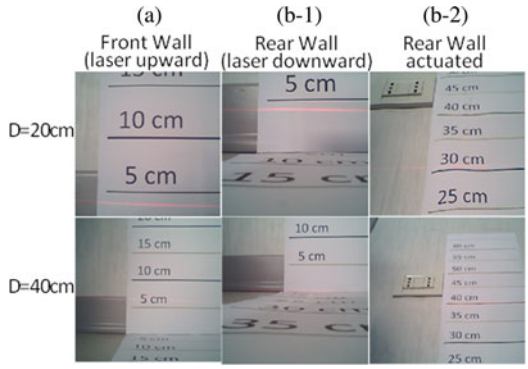

Fig. 7. Captured images from (a) front wall and (b) rear wall.

rear wall showed good performance for detecting small objects or obstacles (e.g., holes) located close to the robot. High objects can be detected also by taking advantage of the bending DoF, when the wall is actuated and lifted as shown in Fig. 7(b-2). For example, when the robot moves autonomously for exploration, it can move putting the front wall in front for far-range sensing or, alternatively, putting the rear wall in front while actuating the wall in order to detect both small and high obstacles. Thanks to the arrangement of the laser-camera sensor (see Fig. 5), the vision system is effective also if the robot is placed upside down.

2) Measurement of Distance: The distance between the robot and a nearby object could be useful for autonomous locomotion and, in some particular cases, can help docking to another robot. As reported in [26], the distance D between the robot and an object (see Fig. 5) can be described as

$$D = \frac{fd}{u + f \cdot \tan(\theta)} \tag{1}$$

where f is the focal length of the camera, d is the distance between the optical center of the camera and the laser, u is the image-plane position where the reflected laser strikes ($u = 0$ at the image-plane center line), and ϑ is the absolute inclination angle of the laser. The parameter f is known for the camera, d and ϑ are the design parameters, and u is the coordinate on the image plane and can be obtained by software after an initial calibration. In the prototype, the laser inclination angle was set as 7°.

3) Image-Guided Locomotion: Different pieces of information about environmental features can be obtained from the integrated laser camera sensor [26]; however, in this study we

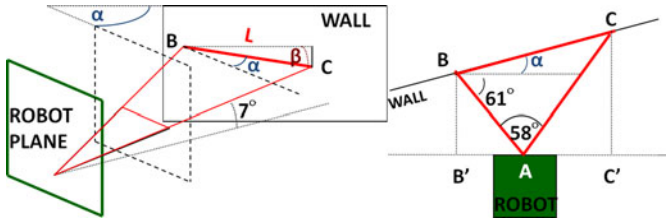

Fig. 8. Scheme of the laser striking an inclined wall.

focused on determining the distance and relative angle between the robot and an obstacle or a wall. Such pieces of information allow the implementation of basic exploration tasks, e.g., obstacle avoidance.

The laser-camera sensor can be used to interact with an obstacle, e.g., a wall, and we can use the information gained as reference for position and orientation of the robot in the space. For instance, if more robots detect the same wall, they can all place themselves at the same distance from such wall and with the same orientation. In this way, since the docking units are centered on all the four lateral walls of the robot—see Section III-E—the docking process would be simplified.

The relative inclination angle α between the robot and an object can be obtained using the inclination angle β of the projected laser line (see Fig. 8). The fan angle of the diffractive optical lens used for the laser was 58°; therefore, the following equations were obtained:

$$\overline{BC} = L\cos(\beta) \tag{2}$$

$$\alpha = \sin^{-1}\left(\frac{(CC' - BB')}{L\cos(\beta)}\right). \tag{3}$$

The length of the projected laser line and distances BB' and CC' can be obtained from captured image information. As regards the accuracy of the system, the error in the distance estimation varies in the range between 1 and 20 mm from the closest detectable object to the farthest, and the resolution is 1 mm at the minimum detectable distance and 12 mm at the maximum range, both in distance and angle estimation since this last feature is derived from the distance itself.

4) Image Processing and Guidance: A camera evaluation board OV7670 EFXA was used to interface the camera to a personal computer, and data acquisition and processing were programmed in LabVIEW to perform sensor-guided locomotion; all the processing was performed off-board. First, the laser line and its edges were extracted by image subtraction of an image snapped with the laser switched ON and the same image with the laser OFF. The image acquisition was synchronized with the laser switching at 10 Hz. Considering the use of the laser-camera sensor, this delay does not limit the possibilities of the Scout robot. The image subtraction principle works appropriately if the environmental illumination condition does not saturate the pixels of the camera and when the background image remains stable (in terms of both illumination and scene) in the time frame of the two consecutive acquisitions.

Fig. 9. Captured image (original) and successfully extracted laser lines.

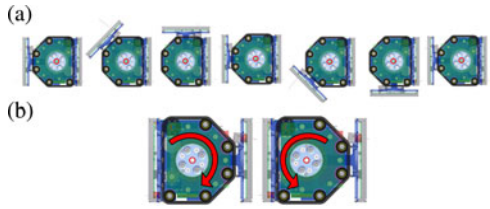

Fig. 10. Two DoFs of the Scout robot: (a) bending DoF and (b) rotational DoF.

In the scenario of autonomous environment exploration, the robot can stop and scan the environment, then, on the basis of the information gained continue exploration.

A LabVIEW IMAQ tool was used for processing the extracted line images. We used a color-based threshold for noise filtering because the laser color was red, and then a low-pass smoothing filter was applied to eliminate noise in the image. Additionally, several IMAQ algorithms were applied including a local thresholding algorithm, gradient convolutions, and erosion-like algorithms, in order to achieve a clearer detection of the laser line; an example of extracted laser lines is shown in Fig. 9. Finally, using the LabVIEW IMAQ particle analysis tool on the processed image, the laser lines' characteristics were extracted and the triangulation algorithms applied. Starting from the obtained pieces of information, the locomotion motors are controlled in order to minimize the error between e.g., the desired predefined distance/orientation with respect to an object and the actual one. The locomotion control is performed using odometry. A maximum error of 5% was experimentally measured due to such technique. However, this value is compatible with the error introduced by the laser camera sensor, which is 3% at maximum range (600 mm, as stated in Section III-C1).

D. 3-D Actuation

The Scout robot has been provided with two actuation units for performing reconfiguration and macrolocomotion of an assembled robotic organism. Two DoFs, named bending and rotation DoFs (see Fig. 10), were implemented. The rotational DoF ($\pm 180^\circ$) allows rotation of the docking unit on the left wall (i.e., with the robot(s) docked to it) as shown in Fig. 10(b). The bending DoF ($\pm 90^\circ$) allows the robot's rear wall to bend as shown in Fig. 10(a). Continuous rotation was deliberately avoided for HW conflict reasons. Moreover, as stated in Section III-A, PCBs are going to be connected to each other in future versions. Therefore, continuous rotation would interfere with these connections. The centers of the actuation axes are

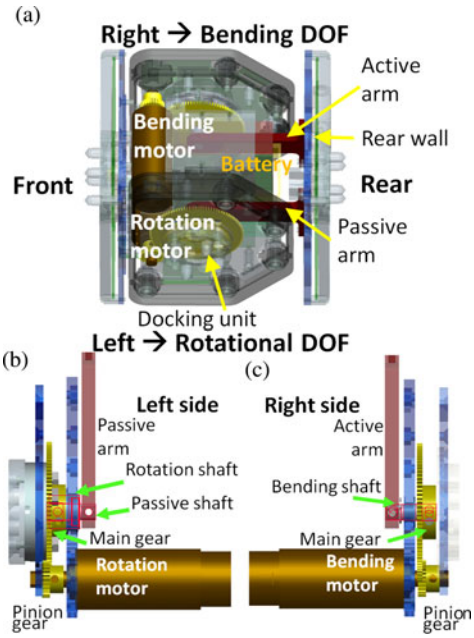

Fig. 11. Design of the actuation units of the Scout robot: (a) overview, (b) rotation DoF mechanism, and (c) bending DoF mechanism.

on the axes that penetrate the robot's center and perpendicular to the robot's walls. This configuration contributes to a smaller computational cost necessary for the control.

Since a compact design was desired, a suitable compromise of torque and dimensions for the actuation motors was selected. Based on these requirements, brushless dc motors (EC 20 flat 351008, Maxon Motor, Switzerland) with gear head of 270:1 reduction ratio (GP22HP 370795, Maxon Motor, Switzerland) have been selected for the bending and rotation DoFs. The design of the actuation units is shown in Fig. 11. The overall diameter of the geared motor is 22 mm, length is 76.1 mm (including the shaft), and nominal output torque is 1 Nm. As regards the transmission mechanism, spur gears with 4:1 reduction ratio were used. Maximum output torque was calculated by assuming that the robots were docked to each other forming a line on a plane, and the robot lifting the docked robots was fixed, for example, to an organism of larger weight. The center of mass for each robot is supposed to be in its geometrical center. The actuation speed was assumed to be slow. The required torque T to lift N robots was estimated as follows:

$$T = \left(\sum_{i=1}^{N} i \right) WL \tag{4}$$

where W is the weight of each module, and L is the length of one robot which is equal to the distance between the centers of two docked robots. Since the maximum output torque after total gear reduction resulted 4.70 Nm, this solution enables the robot to lift up to two other modules. This has been considered satisfying since, as explained in Section II-D, Scout robots are mainly expected to provide sensing capabilities to an assembled organism; however, Scout robots could also autonomously form a little organism, (e.g., five modules) to cross over relatively big obstacles encountered during exploration tasks.

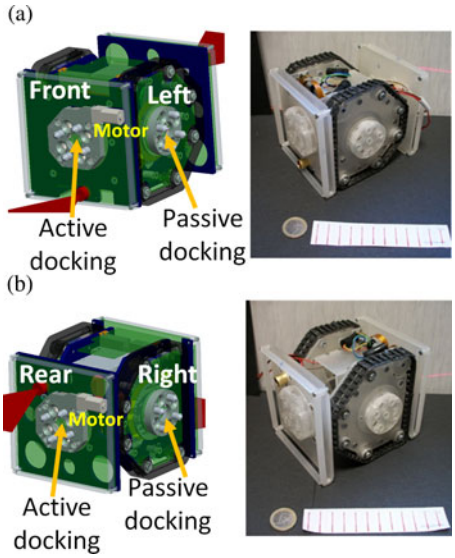

Fig. 12. Overview of the Scout robot—CAD model and real prototype. (a) Front view: details of the docking units on front and left walls. (b) Rear view: details of the docking units on rear and right walls.

In addition, by using motors with such a small diameter, we successfully created a large internal space of 315 cm^3, which was big enough to accommodate battery packs. Actuation motor control was performed using commercial drivers and controllers accompanied with the motors. This procedure was adopted to rapidly and effectively test the robot's performance in assembled configuration.

E. Docking Units

As mentioned in Section II-E, docking and undocking units must be compatible among the three robotic modules shown in Fig. 1(a). The designed docking units are shown in Fig. 12. The design is symmetric and unisex, and each unit has four pins and four holes for docking as well as a central connector for intramodular communication. For docking purposes, the pins inserted in the corresponding holes are blocked all at the same time by an internal gear actuated by a motor (212-404, Precision Microdrives, U.K.) which was embedded into the active docking unit [19]. We also designed a passive docking unit, which has pins, holes, and connector but is not provided with a locking actuation system. The active docking unit can dock both with an active or a passive docking unit. The passive docking unit can be docked to any active docking unit, but not to a passive one.

The docking units must be on the all side walls. However, the docking units on the right and left walls do not need to be activated because the Scout robot cannot move sideways and the docking can be performed if one of the docked units is activated. Moreover, two passive docking units, without actuation units, allow us to save space on the platform. Thus, an easier integration of components is possible. Therefore, a passive docking unit is mounted on right and left wall, respectively, and an active docking unit is mounted on front and rear wall, respectively. In conclusion, the Scout robot has four docking units: one for each side wall, two active and two passive. The docking units are centered on the walls of the robot so that the modules can be docked regardless of orientation.

TABLE I
SPECIFICATION OF THE SCOUT ROBOT PROTOTYPE

Description	Performance
Dimension	105mm×105mm×123mm
Weight	~800g
Locomotion speed	105 mm/s
Track torque	69 mNm
Actuation speed	4.86 rpm
Actuation torque	4 Nm
Bending DoF	± 90°
Rotation DoF	± 180°
Sensors	Two laser-camera sensor units
Docking units	4 in total: 2 active and 2 passive

F. Power Consumption

Since in future versions of the robot all the coding will be implemented on on-board PCBs, the necessary space for PCBs was allocated on the robot (as explained in Section III-A) and the possible power consumption was also considered in the power budget. It was estimated that electronics would consume 5.4 W. The two actuation motors require a total of 6.17 W, while the power consumption of each locomotion motor is 2.34 W. Since two of these motors were implemented in the locomotion units and two in the active docking units, total power consumption is 9.36 W. The power consumption of the sensors is 0.24 W. The overall nominal power consumption of a Scout robot module is 21.17 W. Since the battery implemented on the platform is composed of six-pack lithium batteries with 1400 mAh capacity each (4LI1002, TP electronic components GmbH, Germany), total battery duration of the Scout robot was estimated to be 1.4 h. Obviously, this is an underestimation of the practical duration, since the robot operates in different modes: 2-D locomotion for exploration and docking, and 3-D locomotion for the assembled robotic organism. When the robot performs 2-D locomotion to explore the environment, 3-D actuation is not used, and vice versa; thus, we expect the Scout robot to continue working for several hours.

G. Summary Specifications

The specifications of the designed Scout robot prototype are summarized in Table I for convenience of the readers. As shown in Fig. 2(e), five prototypes were fabricated to conduct experiments and validate basic performance. An overview (front and rear view) of the Scout robot is shown in Fig. 12.

IV. EXPERIMENTS

A. Locomotion Tests

Locomotion performance of the Scout robot was evaluated. Speed of locomotion was experimentally measured to be 105 ± 3 mm/s, which was the same as the theoretical value. This is in

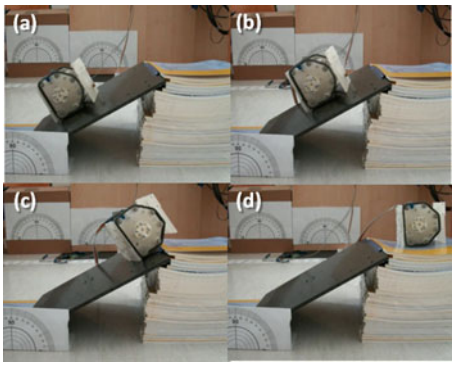

Fig. 13. Scout robot climbing a 40° slope.

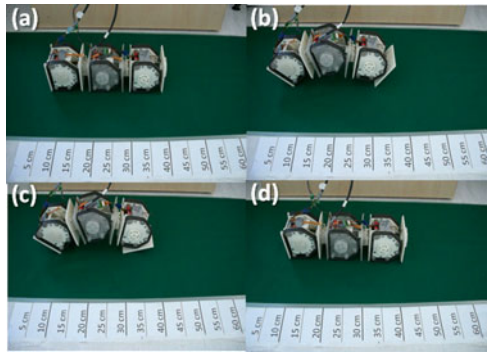

Fig. 15. Frames of the Scout robots performing inchworm locomotion: (a) start position, (b) and (c) robots are performing contraction, and (d) elongation.

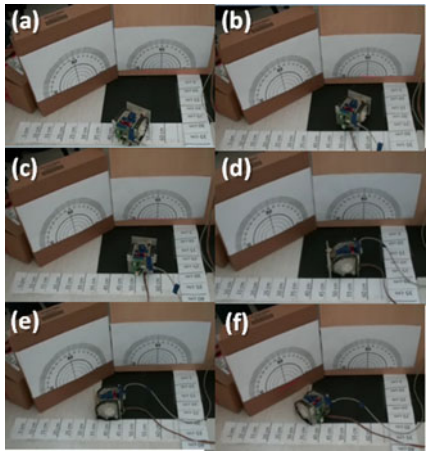

Fig. 14. Image-guided locomotion and exploration of the environment.

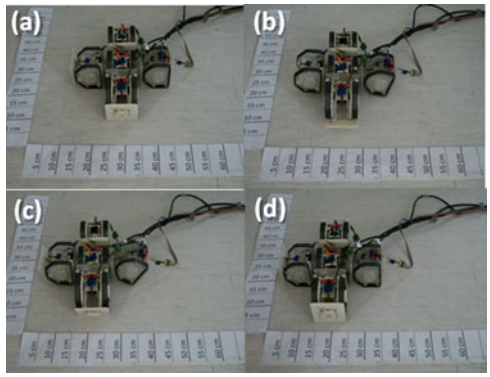

Fig. 16. Scout robots performing four-legged locomotion.

line with performances of other robotic modules in the state of the art such as [27] and [28].

As shown in the sequence of Fig. 13, the Scout robot was able to climb a slope of 40°. The maximum slope that the robot was able to overcome was estimated to be 42°. Such feature can be useful for exploration tasks. Moreover, the reliability of the locomotion unit was tested successfully driving the robot for 1 h continuously.

B. Image-Guided Locomotion

Simple image-guided locomotion of a Scout robot equipped with laser-camera sensor units was tested. The method described in Section III-C was applied to obtain the distance and relative inclination angle to an object. Image-guided locomotion was then performed through simple exploration tasks such as approaching an obstacle and aligning to a wall as shown in Fig. 14. First, the robot calculated its distance from a detected object and approached the obstacle as shown in Fig. 14(a) and (b). Then, the robot calculated its relative inclination to the object, and aligned itself vertically to the object as shown in Fig. 14(c). Thereafter, it rotated around its axis of a predefined quantity searched for another object and successfully aligned itself to the object [see Fig. 14(d)–(f)].

C. Multimode Locomotion

Several locomotion gaits can be performed with an organism composed of Scout robots. In this section, we describe two locomotion patterns that were demonstrated through coordination of the Scout robot DoFs. Locomotion pattern generation and coordination of the actuations must still be developed; however, the mechanical capabilities of the Scout robot were demonstrated as described in the following.

1) Inchworm-Type Mode: The inchworm-type configuration was achieved by using three Scout robot modules manually connected for the test. The locomotion pattern of this configuration was obtained from an inchworm kinematic model [29]. The locomotion cycle was divided into three steps: start position, contraction, and elongation. The locomotion gait of the robotic inchworm was demonstrated as shown in Fig. 15. The speed of locomotion was experimentally measured to be 5 cm/cycle (the same as the theoretical value) which is half of a robot body length per cycle. This is in line with performances of other robotic modules in the state of the art, such as [17], and [30], [31].

2) Quadruped-Walker Mode: Another topology studied for the assembled modules was a quadruped walker. This topology involved five Scout robot modules. The quadruped walker had one module for each leg and a module for the torso (Fig. 16). This robotic organism was able to move in 3-D. The organism was

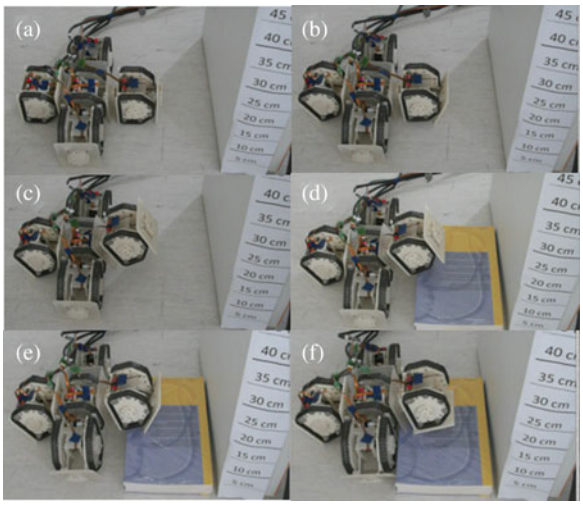

Fig. 17. Quadruped walker overcoming an obstacle.

able to move forward and backward with a locomotion speed of 1 cm per cycle, which is acceptable in this optimization phase.

Although this was much slower than inchworm locomotion, the four-legged organism was able to move in any direction on a 2-D plane. The quadruped walker was able to climb up an obstacle 5 cm high (slope of 90°), as shown in the sequence of Fig. 17. This is something a single Scout robot cannot do. Although the assembled structures tend to move much slower and consume much energy, they could be necessary for tasks in unknown environments. In the scenario of the replicator project, if a swarm of robotic modules were to autonomously explore an environment and encounter problems that cannot be solved with their single functionality, the modules could assemble to form an organism and so extend their capabilities and dexterity. The Scout robot demonstrated that its mechanical function is capable of working in the aforementioned scenario.

V. Conclusion

The Scout robot, a new self-reconfigurable robotic module for autonomous exploration and multimodal locomotion, has been presented together with its design methodology. Scout robot functions, including locomotion, image-guided exploration, and macrolocomotion, were investigated, and the basic mechanical performance was demonstrated using five prototypes.

Scout robot performances can be considered interesting with respect to the state of the art. In fact, even if Scout robot performances are comparable with the performances reported in the literature, such as [17], and [30], [31], the distinguishing feature of this platform is that it is an attempt to bridge a gap between swarm robotics and self-reconfiguring robotics, where technologies are often found as separate research topics.

In the future, we plan to produce a large number of modules to evaluate the overall performance in an assembled state. In addition, we will implement all electronics and software onboard to study the evolution of artificial organisms.

Acknowledgment

The authors would like to thank all members of the REPLICATOR project for fruitful discussions and N. Funaro for his help for robot fabrication.

References

[1] S. Murata, E. Yoshida, A. Kamimura, H. Kurokawa, K. Tomita, and S. Kokaji, "M-TRAN: Self-reconfigurable modular robot," *IEEE/ASME Trans. Mechatronics*, vol. 7, no. 4, pp. 431–441, Dec. 2002.

[2] M. Yim, B. Shirmohammadi, J. Sastra, M. Park, M. Dugan, and C. J. Taylor, "Towards robotic self-reassembly after explosion," in *Proc. IEEE/RJS Int. Conf. Intell. Robots. Syst.*, San Diego, CA, Oct./Nov. 2007, pp. 2767–2772.

[3] M. Yim, K. Roufas, D. Duff, Y. Zhang, C. Eldershawand, and S. Homans, "Modular reconfigurable robots in space applications," *Auton. Robots*, vol. 14, pp. 225–237, 2003.

[4] M. Yim, W.-M. Shen, B. Salemi, D. Rus, M. Moll, H. Lipson, E. Klavins, and G. S. Chirikjian, "Modular self-reconfigurable robot systems," *IEEE Robot. Autom. Mag.*, vol. 14, no. 1, pp. 43–52, Mar. 2007.

[5] R. Groß, M. Bonani, F. Mondada, and M. Dorigo, "Autonomous self assembly in swarm-bots," *IEEE Trans. Robot.*, vol. 22, no. 6, pp. 1115–1130, Dec. 2006.

[6] W.-M. Shen, M. Krivokon, H. Chiu, J. Everist, M. Rubenstein, and J. Venkatesh, "Multimode locomotion via SuperBot robots," in *Proc. IEEE Int. Conf. Robot. Autom.*, Orlando, FL, May 2006, pp. 2552–2557.

[7] S. Murata and H. Kurokawa, "Self-reconfigurable robots," *IEEE Robot. Autom. Mag.*, vol. 14, no. 1, pp. 71–78, Mar. 2007.

[8] S. Tang, Y. Zhu, J. Zhao, and X. Cui, "The UBot modules for self-reconfigurable robot," in *Proc. ASME/IFToMM Int. Conf. Reconfigurable Mech. Robots*, 2009, pp. 529–535.

[9] K. Gilpin and D. Rus, "Modular robot systems," *IEEE Robot. Autom. Mag.*, vol. 17, no. 3, pp. 38–55, Sep. 2010.

[10] M. Yim, Y. Zhang, K. Roufas, D. Duff, and C. Eldershaw, "Connecting and disconnecting for chain self-reconfiguration with PolyBot," *IEEE/ASME Trans. Mechatronics*, vol. 7, no. 4, pp. 442–451, Dec. 2002.

[11] B. Salemi, M. Moll, and W.-M. Shen, "SUPERBOT: A deployable, multifunctional, and modular self-reconfigurable robotic system," in *Proc. IEEE/RSJ Int. Conf. Intell. Robots. Syst.*, Beijing, China, Oct. 2006, pp. 3636–3641.

[12] A. Sproewitz, A. Billard, P. Dillenbourg, and A. Ijspeert, "Roombots—mechanical design of self reconfiguring modular robots for adaptive furniture," in *Proc. IEEE Int. Conf. Robot. Autom.*, Kobe, Japan, May 2009, pp. 4259–4264.

[13] A. Sproewitz, S. Pouya, S. Bonardi, J. Kieboom, R. Möckel, A. Billard, P. Dillenbourg, and A. Ijspeert, "Roombots: Reconfigurable robots for adaptive furniture," *IEEE Comput. Intell. Mag.*, vol. 5, no. 3, pp. 20–32, Aug. 2010.

[14] K. Kotay and D. Rus, "Efficient locomotion for a self-reconfiguring robot," in *Proc. IEEE Int. Conf. Robot. Autom.*, Barcelona, Spain, Apr. 2005, pp. 2963–2969.

[15] A. Golovinsky, M. Yim, Y. Zhang, C. Eldershaw, and D. Duff, "PolyBot and PolyKinetic™ system: A modular robotic platform for education," in *Proc IEEE Int. Conf. Robot. Autom.*, New Orleans, LA, vol. 2, Apr./May 2004, pp. 1381–1386.

[16] A. Castano, A. Behar, and P. M. Will, "The Conro modules for reconfigurable robots," *IEEE/ASME Trans. Mechatronics*, vol. 7, no. 4, pp. 403–409, Dec. 2002.

[17] A. Kamimura, H. Kurokawa, E. Yoshida, S. Murata, K. Tomita, and S. Kokaji, "Automatic locomotion design and experiments for a modular robotic system," *IEEE/ASME Trans. Mechatronics*, vol. 10, no. 3, pp. 314–325, Jun. 2005.

[18] S. Kernbach, O. Scholz, K. Harada, S. Popesku, J. Liedke, H. Raja, W. Liu, F. Caparelli, J. Jemai, J. havlik, E. Meister, and P. Levi, "Multi-robot organisms: State of the art," in *Proc. Int. Conf. Robotics Automation*, (2010), pp. 1–10. [Online]. Available: http://modular.mmmi.sdu.dk/icra10workshop/papers/modular-robots-icra2010-workshop.pdf

[19] S. Kernbach, F. Schlachter, R. Humza, J. Liedke, S. Popesku, S. Russo, T. Ranzani, L. Manfredi, C. Stefanini, R. Matthias, Ch. Schwarzer, B. Girault, P. Alschbach, E. Meister, and O. Scholz, "Heterogeneity for increasing performance and reliability of self-reconfigurable multi-robot organisms," in *Proc. Int. Conf. Intell. Robots Syst. Workshop Reconfigurable Modular Robot.: Challenges*

Mechatronic Bio-Chemo Hybrid Systems, (2011). [Online]. Available: http://www.iros2011.org/WorkshopsAndTutorialsProceedings/SW9/iros_11_sw9_07_final.pdf

[20] H. Wei, Y. Cai, H. Li, D. Li, and T. Wang, "Sambot: A self-assembly modular robot for swarm robot," in *Proc. Int. Conf. Robot. Autom.*, 2010, pp. 66–71.

[21] G. G. Ryland and H. H. Cheng, "Design of iMobot, an intelligent reconfigurable mobile robot with novel locomotion," in *Proc. Int. Conf. Robot. Autom.*, 2010, pp. 60–65.

[22] F. Arvin, K. Samsudin, and M. A. Nasseri, "Design of a differential-drive wheeled robot controller with pulse-width modulation," in *Proc. Innovative Technol. Intell. Syst. Ind. Appl.*, Jul. 2009, pp. 143–147.

[23] W. Wang, H. Zhang, G. Zong, and Z. Deng, "A reconfigurable mobile robots system based on parallel mechanism," in *Parallel Manipulators, Towards New Application*, H. Wu, Ed. Vienna, Austria: I-Tech Education and Publishing, Apr. 2008, pp. 347–362.

[24] R. O'Grady, R. Gross, A. L. Christensen, F. Mondada, M. Bonani, and M. Dorigo, "Performance benefits of self-assembly in a swarm-bot," in *Proc. IEEE/RSJ Int. Conf. Intell. Robots Syst.*, San Diego, CA, Oct. 2007, pp. 2381–2387.

[25] H. B. Brown, Jr., J. M. Vande Weghe, C. A. Bererton, and P. K. Khosla, "Millibot trains for enhanced mobility," In *Proc. IEEE/ASME Trans. Mechatronics*, vol. 7, no. 4, pp. 452–461, Dec. 2002.

[26] G. Fu, P. Corradi, A. Menciassi, and P. Dario, "An integrated triangulation laser scanner for obstacle detection of miniature mobile robots in indoor environment," *IEEE/ASME Trans. Mechatronics*, vol. 16, no. 99, pp. 1–6, Nov. 2010.

[27] J. McLurkin and E. D. Demaine, "A Distributed boundary detection algorithm for multi-robot systems," in *Proc. IEEE/RSJ Int. Conf. Intell. Robots Syst.*, Oct. 2009, pp. 4791–4798.

[28] A. Kamimura, H. Kurokawa, E. Yoshida, K. Tomita, and S. Kokaji, "Distributed adaptive locomotion by a modular robotic system, M-TRAN II from local adaptation to global coordinated motion using CPG controllers national," in *Proc. IEEE/RSJ Int. Conf. Intell. Robots Syst.*, Sendal, Japan, Sep. 28.–Oct. 2, 2004.

[29] Wang, H. X. Zhang, and J. W. Zhang, "Crawling locomotion of modular climbing caterpillar robot with changing kinematic chain," in *Proc. IEEE/RSJ Int. Conf. Intell. Robots Syst.*, St. Louis, MO, Oct. 2009, pp. 5021–5026.

[30] K. Støy, W.-M. Shen, and P. M. Will, "A simple approach to the control of locomotion in self-reconfigurable robots," *Robot. Autonom. Syst.*, vol. 44, pp. 191–199, 2003.

[31] D. Brandt, D. J. Christensen, and H. Hautop Lund, "ATRON robots: Versatility from self-reconfigurable modules," in *Proc. Int. Conf. Mechatronics Autom.*, Harbin, China, Aug. 5–8, 2007, pp. 26–32.

Sheila Russo (S'11) received the Master's degree in biomedical engineering (Hons.) from the University of Pisa, Pisa, Italy, in June 2010. She is currently working toward the Ph.D. degree in biorobotics at the BioRobotics Institute, Scuola Superiore Sant'Anna, Pontedera, Italy.

Her current research interests include medical robotics and biomechatronics.

Kanako Harada (M'06) received the B.E. and M.E. degrees from The University of Tokyo, Tokyo, Japan, and the Ph.D. degree in engineering from Waseda University, Tokyo, in 1999, 2001, and 2007, respectively.

After working for Hitachi, Ltd., Waseda University National Center for Child Health and Development, Scuola Superiore Sant'Anna, and The University of Tokyo, she became a Project Lecturer at The University of Tokyo in 2012. Her research interests include medical and surgical robotics.

Tommaso Ranzani (S'11) received the Master's degree in biomedical engineering (Hons.) from the University of Pisa, Pisa, Italy, in June 2010. He is currently working toward the Ph.D. degree in biorobotics from the BioRobotics Institute, Scuola Superiore Sant'Anna, Pontedera, Italy.

His current research interests include medical robotics and hyper-redundant manipulators.

Luigi Manfredi (M'05) received the Master's degree in computer science engineering from the University of Pisa, Pisa, Italy, and the Ph.D. degree in biorobotics from the Scuola Superiore Sant'Anna, Pontedera, Italy, in 2001 and 2008, respectively.

In 2008, he joined the Center of Research In Microengineering (CRIM LAB), Scuola Superiore Sant'Anna. He is currently a Research Assistant at the Institute of Medical Science and Technology, University of Dundee, Dundee, U.K. His research interests include design and implementation of digital hardware for digital control of multilinked and flexible robots, biorobotics systems, and sensory motor control schemes based on predictive models and/or machine learning.

Cesare Stefanini (M'05) received the Laurea degree in mechanical engineering from the University of Pisa, Pisa, Italy, and the Ph.D. degree in microengineering from the Scuola Superiore Sant'Anna, Pontedera, Italy, in 1997 and 2002, respectively.

He is currently a tenured Assistant Professor at the BioRobotics Institute, Scuola Superiore Sant'Anna. His research interests include small-scale biorobotics, actuators for compliant robots, and micromechatronics. He is the manager of a large-scale European project aimed at developing new high-precision technologies for manufacturing complex shaped parts at the micro/mesoscale level. He has authored or coauthored 27 papers in refereed international journals and more than 50 papers published in international conference proceedings, and holds seven international patents, three of which are currently being applied in industrial micromechatronic products.

Arianna Menciassi (M'02) received the Master's degree in physics (Hons.) from the University of Pisa, Pisa, Italy, and the Ph.D. degree in bioengineering from the Scuola Superiore Sant'Anna, Pontedera, Italy, in 1995 and 1999, respectively.

She is currently an Associate Professor of Biomedical Robotics at the Scuola Superiore Sant'Anna. She has authored or coauthored more than 200 international papers (about 120 in ISI journals) and six book chapters on medical devices and microtechnologies, and holds 25 national and international patents. Her research interests include biomedical micro- and nanorobotics for the development of innovative devices for surgery, therapy, and diagnostics.

Paolo Dario (M'99–SM'01–F'03) received the Master's degree in mechanical engineering from the University of Pisa, Pisa, Italy, in 1977.

He is currently a Professor of Biomedical Robotics at the Scuola Superiore Sant'Anna, Pontedera, Italy, where he supervises a team of about 150 young researchers. He has authored or coauthored more than 300 international papers (about 200 in ISI journals), many international patents, and several book chapters on medical robotics. His research interests include medical robotics, biorobotics, mechatronics, micro/nano engineering, and robotic systems for rehabilitation, prosthetics, surgery, and microendoscopy.

Mr. Dario was a recipient of the Joseph Engelberger Award as a pioneer of biomedical robotics.